

# Nonlinear $\mathcal{H}_\infty$ Control for an Integrated Suspension System via Parameterized Linear Matrix Inequality Characterizations

H.D.Tuan\*, E. Ono†, P. Apkarian‡ and S. Hosoe§

## Abstract

The automotive hydro-pneumatic integrated suspension model is nonlinear with large dimension. As a consequence, the nonlinear  $\mathcal{H}_\infty$  control methodology based on the traditional Hamilton-Jacoby-Isaacs equation is impractical in this application. An alternative so-called Parameterized Linear Matrix Inequality (PLMI) approach is proposed for solving this hard nonlinear  $\mathcal{H}_\infty$  control problem. The validity of the proposed approach is confirmed not only by detailed and realistic simulations but also by extensive experiments. Specifically, the proposed nonlinear control method outperforms the more classical feedback linearization control technique.

**Key words.** Nonlinear  $\mathcal{H}_\infty$  control, Parameterized Linear Matrix Inequalities, Integrated suspension system.

## 1 Introduction

A research area of intense activity in the past five years is certainly the nonlinear  $\mathcal{H}_\infty$  control problem (see e.g. [15, 8]). The central target of nonlinear  $\mathcal{H}_\infty$  control is to internally stabilize the nonlinear plant while minimizing the effect of disturbances such as measurement noise, input disturbances and other exogenous signals which invariably occur in most applications because of plant interactions with the environment. However, in deep contrast with linear  $\mathcal{H}_\infty$  control methods which are flexible, efficient and allow to solve a broad class of linear control problems, there are few practical methods in nonlinear  $\mathcal{H}_\infty$  control which can handle real engineering problems with similar comfort. A prominent obstacle preventing the use of current techniques is that most of them are based on the Hamilton-Jacoby-Isaacs (HJI) equations to characterize solutions. It is well known that with the power of available computers, standard numerical methods for HJI equations are able to solve problems with very low sizes only, say no more than 3 states which rarely suffices for real-world applications. For such hard nonlinear problems, our opinion is that it is of extreme importance to exploit the specific characteristics. It is not doubtful that special structures and properties of a given class of systems will play a crucial role for developing adequate solution methods.

The purpose of the automotive hydro-pneumatic integrated suspension is to improve the ride comfort by oil flow control to cylinder despite bad road environment or vibrations in the human

---

\*Department of Control and Information, Toyota Technological Institute, Hisakata 2-12-1, Tenpaku, Nagoya 468-8511, Japan. Email: tuan@toyota-ti.ac.jp

†Toyota Central Res. & Develop. Labs., Inc., Nagakute, Aichi 480-01, Japan. Email: e-ono@mosk.tytlabs.co.jp

‡ONERA-CERT, 2 av. Edouard Belin, 31055 Toulouse, France. Email: Pierre.Apkarian@cert.fr

§Department of Electronic-Mechanical Engineering, Nagoya University, Furo-cho, Chikusa-ku, Nagoya 464-01, Japan. Email: hosoe@nuem.nagoya-u.ac.jp

sensitivity band. The ride comfort can be enhanced by attenuating vibration of the car body in the human sensitivity band, and therefore,  $\mathcal{H}_\infty$  control with loop-shaping specifications is an effective methodology. The integrated suspension is different from the pure active suspension system [19] by the additional presence of the semi-active valve which exhibits nonlinear characteristics. Thus, the control design for the integrated suspension system becomes inevitably difficult as the resulting model is nonlinear with a large dimension. Therefore, the control design problem here is a very challenging one in nonlinear  $\mathcal{H}_\infty$  control.

Perhaps, the most essential characterization of this control system is that its nonlinearity is caused by the semi-active input. Considering this semi-active input as a parameter, the system can be viewed as a family of parameter-dependent linear systems. It is well known that the linear matrix inequality (LMI) approach is a very efficient and powerful tool to solve various problems for linear systems including linear  $\mathcal{H}_\infty$  problems [6] thanks to the availability of efficient interior-point polynomial-time algorithms for solving semidefinite programming problems [7]. In [2, 18], we have extended the LMI approach to the so-called parameterized LMIs (PLMIs) in order to solve various challenging problems of linear robust control. The purpose of the present paper is to take advantage of these results to solve the nonlinear  $\mathcal{H}_\infty$  control associated with the integrated suspension system. Note that many systems, like the integrated suspension system, with few state variables responsible of the nonlinearity very frequently arise in practical nonlinear models. This was our main motivation for proposing an alternative and practical approach to solve nonlinear  $\mathcal{H}_\infty$  control for such class of systems. The power and efficiency of the proposed method are confirmed by realistic simulations but also by experiments on the physical plant. Particularly, the proposed control is shown to outperforms feedback linearization control and linear control techniques.

The organization of the paper is as follows. Section 2 deals with the model of the integrated suspension system with some preliminary structural analysis. Useful theoretical characterizations involving PLMIs which will constitute our constructive tools are detailed in Section 3. Justification and validation of the approach are shown through simulations and experiments in Section 4. We conclude the paper in Section 5 with some remarks and recommendations for future work.

The notation in the paper is quite standard. Namely,  $M > 0$  or  $M < 0$  for a symmetric matrix  $M$ , means it is negative definite or positive definite. The notation  $M'$  is used for the transpose of the matrix  $M$ .

## 2 Modeling of controlled integrated suspension system

A quarter-car test bench with two degrees of freedom is shown in Fig.1. This system has two control valves. The first one is the active control valve which controls the oil flow from hydraulic pump to suspension cylinder. The second one is the semi-active control valve which controls the cross sectional area of the pipe between cylinder and accumulator. The semi-active valve avails to reduce energy consumption (see e.g. [11] for more details about suspension hydraulic modeling).

The sensitivity band is the limited frequency band within which human is most sensitive and it is assumed to range from 3 to 8Hz (see [19]). With the assumptions that the oil is incompressible, the active control valve and the gas spring characteristics are linearized, the following characterization is obtained.

- The equation for wheel and body motion is [19]:

$$m_1 \ddot{x}_1 = k_t x_{01} - a_p p_c, \quad (1)$$

$$m_2 \ddot{x}_2 = a_p p_c, \quad (2)$$

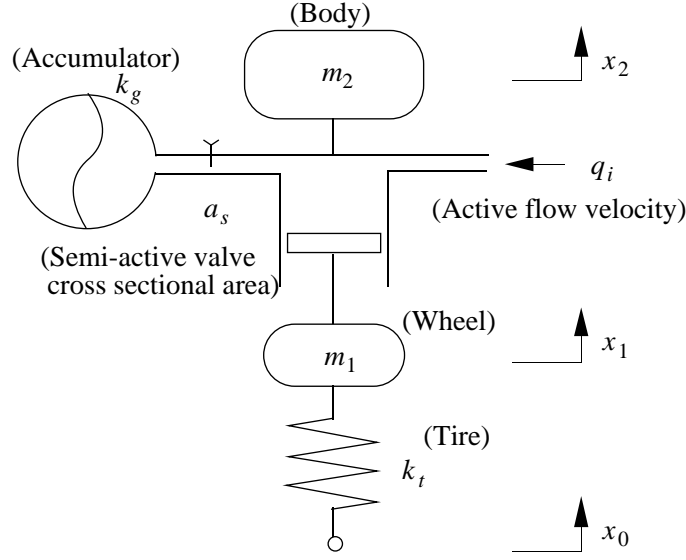


Figure 1: The active suspension system

- The equation for active control flow is:

$$\ddot{q}_i = -\omega_a^2 q_i - 2\eta_a \omega_a \dot{q}_i + k_a \omega_a^2 u_a, \quad (3)$$

- The equation for cylinder pressure deflection is

$$p_c = \frac{k_g}{a_p} x_{12} + \frac{k_g}{a_p^2} v_i + \frac{\rho |a_p (\dot{x}_1 - \dot{x}_2) + q_i| (a_p (\dot{x}_1 - \dot{x}_2) + q_i)}{2c_s^2 a_s^2}. \quad (4)$$

Here, the meaning of variables and parameters is as follows:

- $x_0, x_1, x_2$  are displacement of road, wheel and body,
- $p_c$  is the cylinder pressure deflection,
- $q_i$  is the active control flow,
- $u_a$  is the input command over active control valve,
- $a_s$  is the cross sectional area of semi-active valve,
- $a_p$  is the cross sectional area of cylinder,
- $c_s$  is the semi-active control valve flow coefficient,
- $k_a$  is the active control valve gain,
- $k_g, k_t$  are gas and tire spring constant,
- $m_1, m_2$  are mass of wheel and body,
- $\rho$  is the oil density,
- $\omega_a$  is the natural frequency of active control valve,

- $\eta_a$  is the damping coefficient of active control valve,
- $x_{01}, x_{12}$  and  $\nu_i$  are defined as

$$x_{01} \equiv x_0 - x_1, \quad x_{12} \equiv x_1 - x_2, \quad \nu_i \equiv \int q_i dt.$$

The oil flow in the semi-active valve is defined by

$$\phi(x) = a_p(\dot{x}_1 - \dot{x}_2) + q_i. \quad (5)$$

Take  $u_s$  as the input command over motion of semi-active valve  $a_s$  which is realized via the relation

$$\frac{1}{a_s^2} = \frac{1}{a_{s0}^2}(1 + u_s) \quad (6)$$

where  $a_{s0}$  is some nominal value of  $a_s$ .

According to [19], the ride comfort is defined via human feeling while riding, which is affected by the vibration  $\ddot{x}_2$  of the car body. So  $z_p = \ddot{x}_2$  is chosen as the output to be attenuated. Considering the absolute velocity  $\dot{x}_{01}$  of the road displacement as the disturbance and expressing  $\ddot{x}_2$  accordingly, the integrated suspension model is represented as

$$\begin{aligned} \dot{x}_p &= A_p(\phi)x_p + B_{p1}w + B_{p2}(\phi)u, \\ z_p &= C_p(\phi)x_p + D_p(\phi)u, \end{aligned} \quad (7)$$

where

$$\begin{aligned} x_p &= [x_{01} \quad x_{12} \quad \nu_i \quad \dot{x}_1 \quad \dot{x}_2 \quad q_i \quad \dot{q}_i]' \\ u &= [u_a \quad u_s]' \\ A_p(\phi) &= \begin{bmatrix} 0 & 0 & 0 & -1 & 0 & 0 & 0 \\ 0 & 0 & 0 & 1 & -1 & 0 & 0 \\ 0 & 0 & 0 & 0 & 0 & 1 & 0 \\ a_1 & a_2 & a_3 & a_4 & a_5 & a_6 & 0 \\ 0 & a_7 & a_8 & a_9 & a_{10} & a_{11} & 0 \\ 0 & 0 & 0 & 0 & 0 & 0 & 1 \\ 0 & 0 & 0 & 0 & 0 & a_{12} & a_{13} \end{bmatrix} \\ B_{p1} &= \begin{bmatrix} 1 \\ 0 \\ 0 \\ 0 \\ 0 \\ 0 \\ 0 \end{bmatrix} \quad B_{p2}(\phi) = \begin{bmatrix} 0 & 0 \\ 0 & 0 \\ 0 & 0 \\ 0 & b_1 \\ 0 & b_2 \\ 0 & 0 \\ b_3 & 0 \end{bmatrix} \\ C_p(\phi) &= [0 \quad a_7 \quad a_8 \quad a_9 \quad a_{10} \quad a_{11} \quad 0] \\ D_p(\phi) &= [0 \quad b_2] \end{aligned}$$

and the definitions

$$\begin{aligned}
a_1 &= \frac{k_t}{m_1}, \quad a_2 = -\frac{k_g}{m_1}, \quad a_3 = -\frac{k_g}{m_1 a_p}, \\
a_4 &= -\frac{\rho a_p^2}{2m_1 c_s^2 a_{s0}^2} |\phi(x)|, \quad a_5 = \frac{\rho a_p^2}{2m_1 c_s^2 a_{s0}^2} |\phi(x)|, \\
a_6 &= -\frac{\rho a_p}{2m_1 c_s^2 a_{s0}^2} |\phi(x)|, \quad a_7 = \frac{k_g}{m_2}, \quad a_8 = \frac{k_g}{m_2 a_p}, \\
a_9 &= \frac{\rho a_p^2}{2m_2 c_s^2 a_{s0}^2} |\phi(x)|, \quad a_{10} = -\frac{\rho a_p^2}{2m_2 c_s^2 a_{s0}^2} |\phi(x)|, \\
a_{11} &= \frac{\rho a_p}{2m_2 c_s^2 a_{s0}^2} |\phi(x)|, \quad a_{12} = -\omega_a^2, \quad a_{13} = -2\eta_a \omega_a, \\
b_1 &= -\frac{\rho a_p}{2m_1 c_s^2 a_{s0}^2} |\phi(x)| \phi(x), \quad b_2 = -\frac{\rho a_p}{2m_2 c_s^2 a_{s0}^2} |\phi(x)| \phi(x), \\
b_3 &= k_a \omega_a^2.
\end{aligned} \tag{8}$$

In order to facilitate the design, the above control model can be linearized via the nonlinear transformation (see (48) below)

$$\hat{u}_s = \frac{|\phi(x)| \phi(x)}{|\phi_0|} (1 + u_s) - \phi(x). \tag{9}$$

However, the main drawback of the linearization (9) is that the relationship between control  $\hat{u}_s$  and the semi-active valve input  $a_s$  becomes too complex since it involves the system states and thus the adjustment of  $a_s$  for implementing  $\hat{u}_s$  becomes very delicate. By its actuator nature,  $a_s$  must be limited which means that not any control  $\hat{u}_s$  can be implemented by  $a_s$ . Particularly, with the nonlinear relation (9) even a small value of  $\hat{u}_s$  may cause an arbitrary large value of  $a_s$ , which is unacceptable from the implementation viewpoint. In contrast, the simple relation (6) allows  $a_s$  to be easily adjusted for implementing  $u_s$ . Certainly, (6) requires that  $u_s > -1$  which can be handled through the choice of appropriate weighting functions discussed below. Also  $a_s^2$  is saturated at its maximal value as  $u_s$  approaches  $-1$  from the right (see our experiment result in Section 4).

To achieve improved ride comfort in the human sensitivity band (3 to 8Hz), we introduce the following frequency weighting function for  $z_p$

$$W(s) = \frac{1}{s^2 + 2\zeta\omega_n s + \omega_n^2}, \tag{10}$$

with natural frequency  $\omega_n = 30 \text{ rad/s}$  (4.8Hz) and damping ration  $\zeta = 0.4$ , which leads to the following characterizations (see Fig. 2):

- At low frequency the gain of  $G(s)$  is small (0.003) so in the interval  $1 \sim 2 \text{ Hz}$ , it can efficiently suppress the car body's resonance.
- At the human sensitivity band  $3 \sim 8 \text{ Hz}$  the gain of  $G(s)$  becomes larger with a peak value (0.004) attained at 4.8Hz, to attenuate the vibration of car body for improving the ride comfort.
- Outside the sensitivity band, the gain of  $G(s)$  becomes eventually small to maintain the road holding performance.

The state space representation of function  $W(s)$  is

$$\begin{aligned}
\dot{x}_\omega &= A_\omega x_\omega + B_\omega z_p \\
z_\omega &= C_\omega x_\omega,
\end{aligned} \tag{11}$$

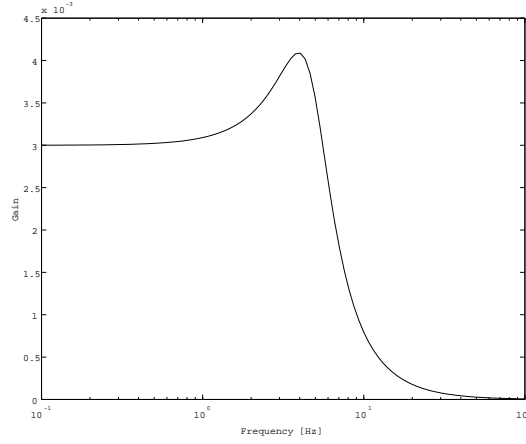


Figure 2: The weighting function

with the numerical data:

$$A_\omega = \begin{bmatrix} 0 & 1 \\ -900 & -24 \end{bmatrix}, \quad B_\omega = \begin{bmatrix} 0 \\ 2.7 \end{bmatrix}, \quad C_\omega = [1 \quad 0].$$

Now, gathering the state-space representations of (7) and (11) and taking the road holding condition and the energy consumption (control input) into account, the generalized plant of our nonlinear problem is rewritten as

$$\begin{aligned} \dot{x} &= A(\phi)x + B_1w + B_2(\phi)u, \\ z &= \begin{bmatrix} Cx \\ Du \end{bmatrix}, \end{aligned} \quad (12)$$

with the notations

$$\begin{aligned} x &= \begin{bmatrix} x_p \\ x_\omega \end{bmatrix}, \quad A(\phi) = \begin{bmatrix} A_p(\phi) & 0 \\ B_\omega C_p(\phi) & A_\omega \end{bmatrix}, \quad B_1 = \begin{bmatrix} B_{p1} \\ 0 \end{bmatrix}, \quad B_2(\phi) = \begin{bmatrix} B_{p2}(\phi) \\ B_\omega D_p(\phi) \end{bmatrix}, \\ C &= \begin{bmatrix} \Omega_c & 0 \\ 0 & C_\omega \end{bmatrix}, \quad D = \begin{bmatrix} \omega_{ac} & 0 \\ 0 & \omega_{se} \end{bmatrix}, \quad \Omega_c = \begin{bmatrix} \omega_{01} & 0 & 0 & 0 & 0 & 0 & 0 \\ 0 & \omega_{12} & 0 & 0 & 0 & 0 & 0 \end{bmatrix}, \end{aligned}$$

and

- $\omega_{01} = 0.2$  is the weighting constant corresponding to road holding performance  $x_{01} = x_0 - x_1$ ;
- $\omega_{12} = 0.03$  is the weighting constant corresponding to car attitude  $x_{12} = x_1 - x_2$ ;
- $\omega_{ac} = 0.0015$  is the weighting constant corresponding to active control input  $u_a$ ;
- $\omega_{se} = 0.0015$  is the weighting constant corresponding to semi-active control input  $u_s$ .

Note that the above values of  $\omega_{01}$ ,  $\omega_{12}$ ,  $\omega_{ac}$  and  $\omega_{se}$  have been chosen through experiments based on the following common trade-offs:

- With  $\omega_{01}$  increased, the road holding performance is improved but then the ride comfort is degraded;
- With  $\omega_{12}$  increased the car attitude performance is improved by suppressing the fluctuation of suspension stroke but then the ride comfort is degraded;

- With  $\omega_{se}$  increased, the semi-active control  $u_s$  becomes smaller and avoids saturation of the semi-active valve  $a_s$  but its ability for improving the ride comfort becomes less efficient. The dependence of the active control  $u_a$  on its weight  $\omega_{ac}$  is similar and moreover there is also a trade-off between semi-active and active controls, as well as between the ride comfort and the energy consumptions  $u_a$  and  $u_s$ . As the later experiments show, due to addition of semi-active control, the ride comfort performance can be achieved with reduced energy consumption.

Now, it becomes clear that our problem of improving the ride comfort is nothing else than a disturbance attenuation problem (i.e.  $\mathcal{H}_\infty$  control). Hereafter, we provide some related mathematical definitions and formulations. A feedback control

$$u = u(x) \quad (13)$$

will be called a  $\gamma$ -gain control if it internally stabilizes the system (12) and the following  $L_2$ -gain condition holds true for the closed-loop system (12)-(13)

$$\int_0^T \|z(t)\|^2 dt \leq \gamma^2 \int_0^T \|w(t)\|^2 dt, \quad \forall T > 0, \quad \forall w \in L_2(0, T) \quad (14)$$

with zero state initial conditions (i.e.  $x(0) = 0$ ). The  $\mathcal{H}_\infty$  control problem for the system (12) is to find a  $\gamma$ -gain control  $u(x)$  with minimal  $\gamma > 0$ .

Clearly, (12) is a nonlinear system with 9 state variables, so the traditional approach based on HJI equation cannot be applied to solve the  $\mathcal{H}_\infty$  control problem. Referring to equations (8), we see that (12) is nonlinear by the presence of the semi-active input  $\phi(x)$  defined by (5). For physical reasons,  $\phi(x)$  cannot take arbitrary values but is restricted in some predefined bounded set  $\mathcal{D}$ . Therefore, it is sufficient to design a control such that both internal stability and  $L_2$ -gain conditions (14) are practically fulfilled, i.e. they have to hold whenever  $\phi(x) \in \mathcal{D}$  only. Therefore, an alternative way to attack the nonlinear  $\mathcal{H}_\infty$  problem for the system (12) is to view the system as a family of linear systems depending on the semi-active input parameter  $\phi(x)$ . Suppose that for every fixed  $\phi \in \mathcal{D}$ , a  $\gamma$ -gain linear control is  $K(\phi)x$  associated with some matrix  $K(\phi)$  and a quadratic Lyapunov function  $x'P(\phi)x$  establishing an  $L_2$ -gain condition. Then, as  $\phi$  is varying as a function of  $x$ , we must find conditions on  $K(\phi(x))$  and on

$$V(x) = x'P(\phi(x))x \quad (15)$$

such that the nonlinear system (12) with control input

$$u = K(\phi(x))x \quad (16)$$

satisfy the  $L_2$ -gain condition (14). It turns out in the next section that such conditions admit a tractable formulation in terms of PLMIs.

Note that function  $V(x)$  might appear restrictive. However, such a form is general enough since the recent max-plus algebra based results [5, 9] show that the value function for a nonlinear system is indeed piecewise quadratic which obviously has a strong connection with the form (15).

### 3 PLMI characterization

In this section, we give a detailed discussion of the solution method used in our problem. First, let us consider the following system

$$\begin{aligned} \dot{x} &= A_{cl}(\phi)x + B_{cl}(\phi)w \\ z &= C_{cl}(\phi)x + D_{cl}(\phi)w, \end{aligned} \quad (17)$$

where for simplicity of notation, we use  $\phi$  for a function  $\phi(t)$  which depends on time  $t$ .

**Lemma 3.1** *The system (17) is internally stable and*

$$\int_0^T \|z\|^2 dt < \gamma^2 \int_0^T \|w\|^2 dt, \quad \forall T > 0, \quad w(\cdot) \in L_2[0, T] \quad (18)$$

if the following matrix inequalities hold true

$$\begin{bmatrix} \dot{X}(\phi) + A'_{cl}(\phi)X(\phi) + X(\phi)A_{cl}(\phi) & X(\phi)B_{cl}(\phi) & C_{cl}(\phi)' \\ B'_{cl}(\phi)X(\phi) & -\gamma I & D'_{cl}(\phi) \\ C_{cl}(\phi) & D_{cl}(\phi) & -\gamma I \end{bmatrix} < 0, \quad (19)$$

$$X(\phi) > 0, \quad (20)$$

where  $\dot{X}(\phi) := \frac{d}{dt}X(\phi(t))$ .

**Proof.** It can be inferred that conditions (19), (20), imply the function  $V(t, x) = x^T X(\phi(t))x$  satisfies the following Hamilton-Jacoby inequality for the gain condition (18)

$$\max_w \left[ \frac{\partial V(t, x)}{\partial t} + \frac{\partial V(t, x)}{\partial x} [A_{cl}(\phi)x + B_{cl}w] + \gamma^{-1}\|z\|^2 - \gamma\|w\|^2 \right] < 0 \quad (21)$$

(see e.g. [1, 3, 20] for related issues).  $\square$

Now, step back to the nonlinear system (12). Suppose that we seek a feedback control in the form (16), then the closed-loop system can be represented in the form (17) with

$$A_{cl}(\phi) = A(\phi) + B_2(\phi)K(\phi), \quad B_{cl}(\phi) = B_1(\phi), \quad C_{cl}(\phi) = C_1 + D_{12}K(\phi), \quad D_{cl}(\phi) = 0, \quad (22)$$

where

$$C_1 = \begin{bmatrix} C \\ 0 \end{bmatrix}, \quad D_{12} = \begin{bmatrix} 0 \\ D \end{bmatrix}.$$

The inequality (19) of Lemma 3.1 reads

$$\begin{aligned} & \begin{bmatrix} \dot{X}(\phi) + [A(\phi) + B_2(\phi)K(\phi)]^T X(\phi) \\ \quad + X(\phi)[A(\phi) + B_2(\phi)K(\phi)] & X(\phi)B_1 & [C_1 D_{12}K(\phi)]^T \\ B'_1 X(\phi) & -\gamma I & 0 \\ C_1 + D_{12}K(\phi) & 0 & -\gamma I \end{bmatrix} < 0 \\ \Leftrightarrow & \begin{bmatrix} -\dot{P}(\phi) + P(\phi)A^T(\phi) + R(\phi)^T B_2^T(\phi) \\ \quad + A(\phi)P(\phi) + B_2(\phi)R(\phi) & B_1 & P(\phi)C_1^T + R(\phi)^T D_{12}^T \\ B'_1 & -\gamma I & 0 \\ C_1 P(\phi) + D_{12}R(\phi) & 0 & -\gamma I \end{bmatrix} < 0, \\ & 0 < P(\phi) = X^{-1}(\phi), \quad \frac{d}{dt}P(\phi) = -X(\phi)^{-1}\dot{X}(\phi)X(\phi)^{-1}, \quad R(\phi) = K(\phi)X(\phi) \end{aligned} \quad (23)$$

$$\begin{aligned} \Leftrightarrow & \begin{bmatrix} -\dot{P}(\phi) + P(\phi)A^T(\phi) + A(\phi)P(\phi) & B_1 & P(\phi)C_1^T \\ B'_1 & -\gamma I & 0 \\ C_1 P(\phi) & 0 & -\gamma I \end{bmatrix} \\ & + \begin{bmatrix} B_2(\phi) \\ D_{12} \\ 0 \end{bmatrix} R(\phi) \begin{bmatrix} I & 0 & 0 \end{bmatrix} + \begin{bmatrix} I \\ 0 \\ 0 \end{bmatrix} R^T(\phi) \begin{bmatrix} B_2^T(\phi) & D_{12}^T & 0 \end{bmatrix} < 0 \end{aligned} \quad (24)$$

By an immediate application of the Finsler's Lemma [4], (24) is in turn equivalent to the existence of a scalar  $\sigma$  such that

$$\begin{aligned} & \begin{bmatrix} -\dot{P}(\phi) + P(\phi)A^T(\phi) + A(\phi)P(\phi) & P(\phi)C_1^T & B_1 \\ C_1 P(\phi) & -\gamma I & 0 \\ B'_1 & 0 & -\gamma I \end{bmatrix} \\ & -\sigma \begin{bmatrix} B_2(\phi) \\ D_{12} \\ 0 \end{bmatrix} \begin{bmatrix} B_2^T(\phi) & D_{12}^T & 0 \end{bmatrix} < 0 \end{aligned} \quad (25)$$



Furthermore, using a standard least square technique and noting that the matrix  $D_{12}$  is full column rank, a particular solution  $K$  is given as

$$K(\phi) = -(D'_{12}D_{12})^{-1}[D'_{12}C_1 + \gamma B_2(\phi)'P(\phi)^{-1}]. \quad (26)$$

The reader is referred to [1] and references therein for more details. Thus our focus now becomes to solving the differential inequality (25), which is still a difficult problem. To the aim of simplifying this problem, we shall examine some approximated representations of  $P(\phi)$ . Looking at the nonlinear system (12), we see that the nonlinear terms  $A(\phi)$  and  $B_2(\phi)$  can be expressed as

$$A(\phi) = A_0 + |\phi|A_1, \quad B_2(\phi) = B_{20} + |\phi|B_{21} \quad (27)$$

where  $A_0, A_1, B_{20}, B_{21}$  are constant matrices.

The structure (27) suggests to seek a solution  $P(\phi)$  of the inequality (24) in the ad-hoc basis

$$P(\phi) = P_0 + |\phi|P_1 + |\phi|\phi P_2, \quad (28)$$

and thus

$$\dot{P}(\phi) = \begin{cases} \dot{\phi}(t)P_1 + 2\dot{\phi}(t)\phi P_2 & \text{if } \phi \geq 0 \\ -\dot{\phi}(t)P_1 - 2\dot{\phi}(t)\phi P_2 & \text{if } \phi \leq 0 \end{cases} \quad (29)$$

Note that  $P(\phi)$  may be not differentiable at  $\phi = 0$  but this does not cause any trouble in this application.

Now, restricting  $(\dot{\phi}, \phi)$  on the area  $M \times [-m_0, m_0]$  with  $M \subset \mathbb{R}$  bounded and  $0 < m_0 \leq 1$  ( $\phi$  in (5) is the oil flow in semi-active valve so such kind of restriction is rather natural) which can be done by changing  $A_1, B_{21}$  in (27) if necessary, and with the notation  $\mathcal{P} := (P_0, P_1, P_2)$ ,  $\theta := \dot{\phi}$ , we can rewrite (25) in the form

$$M_0(\mathcal{P}) + \theta M_{01}(\mathcal{P}) + \theta\phi M_{02}(\mathcal{P}) + \phi M_1(\mathcal{P}) + \phi^2 M_2(\mathcal{P}) + \phi^3 M_3(\mathcal{P}) + \phi^4 M_4 < 0, \quad \forall(\theta, \phi) \in M \times [0, m_0], \quad (30)$$

$$M_0(\mathcal{P}) - \theta M_{01}(\mathcal{P}) - \theta\phi M_{02}(\mathcal{P}) - \phi M_1(\mathcal{P}) + \phi^2 \bar{M}_2(\mathcal{P}) + \phi^3 M_3(\mathcal{P}) + \phi^4 M_4 < 0, \quad \forall(\theta, \phi) \in M \times [-m_0, 0]. \quad (31)$$

with the definitions

$$\begin{aligned} M_0(\mathcal{P}) &= \begin{bmatrix} P_0 A'_0 + A_0 P_0 & P_0 C'_1 & B_1 \\ C_1 P_0 & -\gamma I & 0 \\ B'_1 & 0 & -\gamma I \end{bmatrix} - \sigma \begin{bmatrix} B_{20} B'_{20} & B_{20} D'_{12} & 0 \\ D_{12} B'_{20} & D_{12} D'_{12} & 0 \\ 0 & 0 & 0 \end{bmatrix}, \\ M_{01}(\mathcal{P}) &= - \begin{bmatrix} P_1 & 0 & 0 \\ 0 & 0 & 0 \\ 0 & 0 & 0 \end{bmatrix}, \quad M_{02}(\mathcal{P}) = -2 \begin{bmatrix} P_2 & 0 & 0 \\ 0 & 0 & 0 \\ 0 & 0 & 0 \end{bmatrix}, \\ M_1(\mathcal{P}) &= \begin{bmatrix} P_0 A'_1 + A_1 P_0 + P_1 A'_0 + A_0 P_1 & P_1 C'_1 & 0 \\ C_1 P_1 & 0 & 0 \\ 0 & 0 & 0 \end{bmatrix}, \\ M_{11}(\mathcal{P}) &= \begin{bmatrix} P_2 A'_0 + A_0 P_2 & P_2 C'_1 & 0 \\ C_1 P_2 & 0 & 0 \\ 0 & 0 & 0 \end{bmatrix} - \sigma \begin{bmatrix} B_{21} B'_{20} + B_{20} B'_{21} & B_{21} D'_{12} & 0 \\ D_{12} B'_{21} & 0 & 0 \\ 0 & 0 & 0 \end{bmatrix}, \\ M_{20}(\mathcal{P}) &= \begin{bmatrix} P_1 A'_1 + A_1 P_1 & 0 & 0 \\ 0 & 0 & 0 \\ 0 & 0 & 0 \end{bmatrix}, \\ M_2(\mathcal{P}) &= M_{11}(\mathcal{P}) + M_{20}(\mathcal{P}), \quad \bar{M}_2(\mathcal{P}) = M_{20}(\mathcal{P}) - M_{11}(\mathcal{P}), \\ M_3(\mathcal{P}) &= \begin{bmatrix} P_2 A'_1 + A_1 P_2 & 0 & 0 \\ 0 & 0 & 0 \\ 0 & 0 & 0 \end{bmatrix}, \quad M_4 = -\sigma \begin{bmatrix} B_{21} B'_{21} & 0 & 0 \\ 0 & 0 & 0 \\ 0 & 0 & 0 \end{bmatrix}. \end{aligned} \quad (32)$$

Let us rewrite (31) in the more compact form

$$\begin{aligned} \bar{M}_0(\mathcal{P}) + \theta \bar{M}_{01}(\mathcal{P}) + \theta \phi \bar{M}_{02}(\mathcal{P}) + \phi \bar{M}_1(\mathcal{P}) \\ + \phi^2 \bar{M}_2(\mathcal{P}) + \phi^3 \bar{M}_3(\mathcal{P}) + \phi^4 \bar{M}_4 \end{aligned} < 0, \quad \forall (\theta, \phi) \in M \times [0, m_0]. \quad (33)$$

with the definitions

$$\begin{aligned} \bar{M}_0(\mathcal{P}) = M_0(\mathcal{P}), \quad \bar{M}_{01}(\mathcal{P}) = -M_{01}(\mathcal{P}), \quad \bar{M}_{02}(\mathcal{P}) = M_{02}(\mathcal{P}), \\ \bar{M}_1(\mathcal{P}) = M_1(\mathcal{P}), \quad \bar{M}_3(\mathcal{P}) = -M_3(\mathcal{P}), \quad \bar{M}_4 = M_4. \end{aligned} \quad (34)$$

Analogously, the positive definiteness of  $P(\phi)$

$$P_0 + |\phi|P_1 + |\phi|\phi P_2 > 0, \quad \forall \phi \in [-m_0, m_0]$$

is rewritten as

$$P_0 + \phi P_1 + \phi^2 P_2 > 0, \quad \forall \phi \in [0, m_0], \quad (35)$$

$$P_0 + \phi P_1 - \phi^2 P_2 > 0, \quad \forall \phi \in [0, m_0]. \quad (36)$$

Summing up, we have to solve (30), (35) and (31), (36) which constitute a set of PLMIs, since for every fixed values of  $(\theta, \phi)$ , they just become standard LMIs. The difficulty of solving PLMIs is that they involve infinitely many LMIs. In [2, 18], it has been shown how to convert, possibly conservatively, PLMIs into a finite number of LMIs by using different variants of extreme point results or convex majorization techniques. The following result is important in that respect.

**Lemma 3.2** *One has, for all  $x$  and  $M_i(\mathcal{P})$*

$$\phi^i x' M_i(\mathcal{P}) x \leq g_{ix}(\phi) := \max\{\phi^i x' M_i(\mathcal{P}) x, (\frac{i m_0^{i-1}}{2^{i-1}} \phi - \frac{i-1}{2^i} m_0^i) x' M_i(\mathcal{P}) x\} \quad (37)$$

whenever  $\phi \in [0, m_0]$  and  $i \geq 2$ .

**Proof.** We have

$$\phi^i \geq \frac{i m_0^{i-1}}{2^{i-1}} \phi - \frac{i-1}{2^i} m_0^i, \quad \forall \phi \in [0, m_0] \quad (38)$$

since the the function in the right hand size of (38) is the tangent to the curve  $\phi^i$  at  $m_0/2$ . Thus

$$\begin{aligned} \phi^i x' M_i(\mathcal{P}) x &\geq (\frac{i m_0^{i-1}}{2^{i-1}} \phi - \frac{i-1}{2^i} m_0^i) x' M_i(\mathcal{P}) x \quad \text{whenever } x' M_i(\mathcal{P}) x \geq 0 \\ \phi^i x' M_i(\mathcal{P}) x &\leq (\frac{i m_0^{i-1}}{2^{i-1}} \phi - \frac{i-1}{2^i} m_0^i) x' M_i(\mathcal{P}) x \quad \text{whenever } x' M_i(\mathcal{P}) x \leq 0 \end{aligned}$$

and (37) follows.  $\square$

Note that function  $\phi^i x' M_i(\mathcal{P}) x$  is convex or concave on  $\phi$  depending on the sign of  $x' M_i(\mathcal{P}) x$ . However, function  $g_{ix}$  is always convex in  $\phi$  since

$$g_{ix}(\phi) = \begin{cases} x' M_i(\mathcal{P}) x \phi^i & \text{if } x' M_i(\mathcal{P}) x \geq 0 \\ -x' M_i(\mathcal{P}) x (\frac{i m_0^{i-1}}{2^{i-1}} \phi - \frac{i-1}{2^i} m_0^i) & \text{if } x' M_{ij} x \leq 0 \end{cases} \quad (39)$$

and both functions  $\phi^i$  and  $(\frac{i m_0^{i-1}}{2^{i-1}} \phi - \frac{i-1}{2^i} m_0^i)$  are convex on  $[0, m_0]$ . The convexity of  $g_{ix}$  plays an important role in the subsequent developments.

Since  $M_4$  is negative semidefinite, by (37) one has

$$\phi^4 x' M_4 x \leq (0.5 m_0^3 \phi - 0.1875 m_0^4) x' M_4 x \quad (40)$$

In view of (37) and (40),

$$\begin{aligned} & x'[M_0(\mathcal{P}) + \theta M_{01}(\mathcal{P}) + \theta\phi M_{02}(\mathcal{P}) + \phi M_1(\mathcal{P}) + \phi^2 M_2(\mathcal{P}) + \phi^3 M_3(\mathcal{P}) + \phi^4 M_4]x \leq \\ & x'[M_0(\mathcal{P}) + \theta M_{01}(\mathcal{P}) + \theta\phi M_{02}(\mathcal{P}) + \phi M_1(\mathcal{P})]x + \\ & \max\{\phi^2 x' M_2(\mathcal{P})x, (m_0\phi - 0.25m_0^2)x' M_2(\mathcal{P})x\} + \\ & \max\{\phi^3 x' M_3(\mathcal{P})x, (0.75m_0^2\phi - 0.25m_0^3)x' M_3(\mathcal{P})x\} + (0.5m_0^3\phi - 0.1875m_0^4)x' M_4x \end{aligned}$$

and thus (30) is fulfilled if

$$\begin{aligned} & x'[M_0(\mathcal{P}) + \theta M_{01}(\mathcal{P}) + \theta\phi M_{02}(\mathcal{P}) + \phi M_1(\mathcal{P})]x + \\ & \max\{\phi^2 x' M_2(\mathcal{P})x, (m_0\phi - 0.25m_0^2)x' M_2(\mathcal{P})x\} + \\ & \max\{\phi^3 x' M_3(\mathcal{P})x, (0.75m_0^2\phi - 0.25m_0^3)x' M_3(\mathcal{P})x\} + \\ & (0.5m_0^3\phi - 0.1875m_0^4)x' M_4x < 0 \end{aligned} \quad (41)$$

for all  $x \neq 0$  and  $\phi \in [0, m_0]$ .

Furthermore, since the left-hand side of (41) is a convex function of  $\phi$  which implies that its maximum over  $[0, m_0]$  must be attained on  $\{0, m_0\}$  with fixed  $\theta \in M$ . Analogously, the maximum of left-hand side of (41) must be attained on the set  $\text{vert}M$  of all vertices of  $M$  with fixed  $\phi \in [0, m_0]$ . Hence, it is deduced that the maximum of the left hand side of (41) must be attained on  $\text{vert}M \times [0, m_0]$ . Thus, to check (41) on  $M \times \phi \in [0, m_0]$ , it is sufficient to check the inequality on the finite cardinality set  $(\theta, \phi) \in \text{vert}M \times \{0, m_0\}$ . Then (41) becomes an LMI problem. For simplicity let us use the following notation to refer to (41) for  $(\theta, \phi) \in \text{vert}M \times \{0, m_0\}$ ,

$$\begin{aligned} & M_0(\mathcal{P}) + \theta M_{01}(\mathcal{P}) + \theta\phi M_{02}(\mathcal{P}) + \phi M_1(\mathcal{P}) + \\ & \max\{\phi^2 M_2(\mathcal{P}), (m_0\phi - 0.25m_0^2)M_2(\mathcal{P})\} + \\ & \max\{\phi^3 M_3(\mathcal{P}), (0.75m_0^2\phi - 0.25m_0^3)M_3(\mathcal{P})\} + \\ & (0.5m_0^3\phi - 0.1875m_0^4)M_4 < 0 \end{aligned} \quad (42)$$

With similar notations, (35), (33) and (36) hold if

$$P_0 + \phi P_1 + \min\{\phi^2 P_2, (m_0\phi - 0.25m_0^2)P_2\} > 0 \quad (43)$$

$$\begin{aligned} & \bar{M}_0(\mathcal{P}) + \theta \bar{M}_{01}(\mathcal{P}) + \theta\phi \bar{M}_{02}(\mathcal{P}) + \phi \bar{M}_1(\mathcal{P}) + \\ & \max\{\phi^2 \bar{M}_2(\mathcal{P}), (m_0\phi - 0.25m_0^2)\bar{M}_2(\mathcal{P})\} + \\ & \max\{\phi^3 M_3(\mathcal{P}), (0.75m_0^2\phi - 0.25m_0^3)M_3(\mathcal{P})\} + (0.5m_0^3\phi - 0.1875m_0^4)M_4 < 0 \end{aligned} \quad (44)$$

$$P_0 + \phi P_1 + \min\{-\phi^2 P_2, -(m_0\phi - 0.25m_0^2)P_2\} > 0 \quad (45)$$

$$\forall (\theta, \phi) \in \text{vert}M \times \{0, m_0\},$$

Finally, the LMIs (42)-(45) constitute a sufficient condition for the existence of a  $\gamma$ -gain controller of the form (16). Using the solutions  $P_0, P_1, P_2$  of (42)-(45), the matrix function  $K(\phi)$  can be easily computed by using the formula (26).

**Remark.** Clearly, we can modify the representation (28) as

$$P(\phi) = \begin{cases} P_0 + \phi P_1 + \phi^2 P_2 & \text{if } \phi \geq 0 \\ P_0 - \phi \bar{P}_1 - \phi^2 \bar{P}_2 & \text{if } \phi \leq 0 \end{cases} \quad (46)$$

to get more freedom and improved performance because of the additional variables  $\bar{P}_1$  and  $\bar{P}_2$ . Then accordingly,  $\bar{P}_1$  and  $\bar{P}_2$  replace  $P_1, P_2$  respectively in (44)-(45). Using the viscosity solution approach (see e.g. [8]) it is easy to show that such a  $P(\phi)$  defined by (46) satisfying (42)-(45) indeed yields  $\gamma$ -gain controllers.

In [17] we have also developed a result for  $\mathcal{H}_\infty$  control for a class of bilinear systems. The approach of [17] has been based on the single quadratic Lyapunov rather than parameter-dependent Lyapunov functions presented here. Clearly, system (12) is not bilinear and even the single Lyapunov function based approach will result in a PLMI as well.

## 4 Experimental results

The controller developed in Section 3 is implemented with a sample period of 5 ms. A hydraulic shaker simulates road disturbance generated by driving at 50 km/h. For solving the LMIs (42)-(45), we use the MATLAB LMI Control Toolbox [7].

The performance of our nonlinear control can be assessed by comparing its performance with other design methods such as:

- Control with passive suspension having constant damping coefficient,
- Linear  $\mathcal{H}_\infty$  control for the feedback linearized model of (12) [10, 15, 16].

The passive suspension condition can be realized in our apparatus, by adjusting the semi-active valve according to

$$a_s = a_{s0} \sqrt{\frac{a_p |\dot{x}_1 - \dot{x}_2|}{|\phi_0|}}, \quad (47)$$

where  $\phi_0$  is the coefficient determining the damping ratio.

On the other hand, if we use the nonlinear transformation (9), then  $p_c$  in (4) can be expressed as

$$p_c = \frac{k_g}{a_p} x_{12} + \frac{k_g}{a_p^2} v_i + \frac{\rho |\phi_0|}{2c_s^2 a_{s0}^2} \{a_p (\dot{x}_1 - \dot{x}_2) + q_i\} + \frac{\rho |\phi_0|}{2c_s^2 a_{s0}^2} \hat{u}_s$$

Consequently, all  $a_i$ 's and also  $b_1$  in (8) are independent of  $\phi(x)$ , while  $b_2, b_3$  are linearly dependent on  $\phi(x)$ , so the transformed model of the plant (12) becomes the following exactly linearized model

$$\begin{aligned} \dot{x} &= A(\phi_0)x + B_1 w + B_2(\phi_0)\hat{u}, \\ z &= \begin{bmatrix} Cx \\ D\hat{u} \end{bmatrix}, \end{aligned} \quad (48)$$

where

$$\hat{u} = [u_a \quad \hat{u}_s]'$$

Note that the parameters in (9) are chosen so that matrix  $A$  in (48) and for the passive suspension system coincide. Also, the same weighting function is used both for the linear and the nonlinear  $\mathcal{H}_\infty$  control. The linear  $\mathcal{H}_\infty$  control theory is readily applied to solve the  $\mathcal{H}_\infty$  control problem for system (48).

The frequency responses in Fig.3 and Fig. 4 represent the ratio of the Fast Fourier Transformations (FFT) for the road displacement and body accelerations. Fig.3 shows simulation results with impulse road displacement (height=0.03 m) and Fig.4 shows experimental results with random road displacement which expresses actual road surface (driving at 50 km/h). The time responses of the random road displacement and body acceleration with the nonlinear  $\mathcal{H}_\infty$  controller are shown in Fig. 5. The control effect at human sensitivity frequency band (3 ~ 8 Hz) and lower frequencies are indicated in Fig.3 and 4. Clearly, the control effect of the nonlinear  $\mathcal{H}_\infty$  control at frequencies lower than 5 Hz is better than that of the linear  $\mathcal{H}_\infty$  control for the feedback linearized system (48).

As mentioned in Section 2, since the value of semi-active valve  $a_s$  is limited, in practical implementation, we have to saturate  $a_s$  at its maximal value when it becomes over-limited which may cause troublesome fluctuations of  $a_s$ . By (6)

$$a_s = \frac{a_{s0}}{\sqrt{1 + u_s}} \quad (49)$$

and thus such fluctuation can be avoided by making the nonlinear  $\mathcal{H}_\infty$  control  $u_s$  reasonably small which is possible due to the appropriate weighting constant  $\omega_{se}$ . In contrast, with (47)

or (9) in the case of passive suspension and feedback linearization control, such fluctuation is unavoidable:  $a_s$  is passive in (9) and  $a_s$  may be over-limited even if  $u_s$  is sufficiently small in (9). Fig. 6 and Fig. 7 showing the active valve flow velocities and semi-active valve cross sectional area after step disturbances clarify this fact. The control inputs of the nonlinear  $\mathcal{H}_\infty$  control (Fig.6) shows stable responses and  $a_s$  is instantly suppressed. However, semi-active control input of the linear  $\mathcal{H}_\infty$  control for the feedback linearized model (Fig. 7) which includes nonlinear variable transformation shows unstable responses even if active control input (being directly controlled) shows stable response:  $a_s$  is fluctuated and frequently suppressed.

Fig. 8 and Fig. 9 display the ride comfort and control inputs with changing weighting constant  $\omega_{se}$  corresponding to semi-active control input from 0.0015 down to 0.0005. The frequency response characteristics demonstrate that the ride comfort can be improved by decreasing the weighting constant corresponding to the semi-active control input. In Fig. 9, the magnitude of semi-active control input becomes increasing and the magnitude of active control becomes decreasing with changing weighting constant. Hence, the oil flow which is necessary for active control becomes decreasing and energy consumption goes down.

Fig. 10 shows a comparison of control performance between our integrated suspension and the pure active suspension [19]. The pure active suspension has a constant damping coefficient and the controller is designed by linear  $\mathcal{H}_\infty$  control [16]. The integrated suspension and the pure active suspension have almost the same control performance. However, the energy consumption of the integrated suspension is better than pure active suspension as indicated in Fig 11. This shows that the semi-active valve avails to reduce the energy consumption.

Finally, the semi-active control is an effective tool for the improvement of the ride comfort with a reasonable energy consumption and this has direct beneficial consequences for the design of more efficient car control systems.

## 5 Conclusion

In this paper, we have considered the nonlinear  $\mathcal{H}_\infty$  control problem of an integrated suspension system. A novel approach has been proposed in this context. It is based on a PLMI characterization which provides sufficient conditions for closed-loop stability and performance of the nonlinear system. The main thrust of this approach, which is seemingly absent in many existing methodologies, is that it allows to solve nonlinear problems with large state dimensions. The only limitation appears to be the number of nonlinearities involved in the model description. When compared to more traditional techniques, it appears that the additional cost required for solving PLMI problems is more than offset by the advantages provided by the technique in terms of augmented stability and improved performance. This has been showed by a fairly complete set of simulations and experiments which finally more than anything else advocate for the use of the proposed method.

**Acknowledgements.** The authors are grateful to the associate editor Dr. Kevin A. Wise and two anonymous reviewers for very helpful comments which have helped to improved the presentation of this paper.

## References

- [1] P. Apkarian, R. J. Adams (1997), Advanced Gain-Scheduling Techniques for Uncertain Systems, *IEEE Trans. on Control System Technology*, vol. 6, 1, pp 21-32
- [2] P. Apkarian, H.D. Tuan, Parameterized LMIs in control theory, *Proc. of 37th CDC*, 1998, 152-157; To appear in *SIAM J. Control and Optimization*.

- [3] G. Becker, A. Packard, Robust performance of linear parametrically varying systems using parametrically-dependent linear feedback, *Systems & Control Letters* 23(1994), 205-215.
- [4] S. Boyd, L. ElGhaoui, E. Feron, V. Balakrishnan (1994), *Linear Matrix Inequalities in Systems and Control Theory*, SIAM Studies in Applied Mathematics, Philadelphia.
- [5] W.H. Fleming, W.M. McEneaney, A max-plus based algorithm for an HJB equation of nonlinear filtering, *Submitted*.
- [6] Gahinet, P. and P. Apkarian (1994). A linear matrix inequality approach to  $\mathcal{H}_\infty$  control. *Int. J. Robust Nonlinear Contr.* 4, 421-448.
- [7] P. Gahinet, A. Nemirovski, A.J. Laub, M. Chilali (1994), *LMI Control Toolbox*, The Math-Works Inc..
- [8] J.W. Helton, M. James, *Extending  $H_\infty$  control to nonlinear systems*, SIAM Frontier in Applied Mathematics, 1999.
- [9] M. Horton, W.L. McEneaney, Max-plus eigenvector representations for nonlinear  $H_\infty$  value functions, *Proc. of 1999 American Control Conference*, 1400-1404.
- [10] A. Isidori, *Nonlinear control systems*, Springer, 1989.
- [11] H.E. Merritt, *Hydraulic control systems*, John Wiley & Sons, 1991.
- [12] E. Ono, K. Takanami, N. Iwama, Y. Hayashi, Y. Hirano, Y. Satoh (1994), Vehicle integrated control for steering and traction systems by  $\mu$  synthesis, *Automatica* 30, 1639-1647.
- [13] E.Ono, S.Hosoe, H.D.Tuan and Y.Hayashi (1996) Nonlinear  $\mathcal{H}_\infty$  control of active suspension, *Vehicle System Dynamics Supplement* 25, 489-501.
- [14] E. Ono, S. Hosoe, H.D. Tuan, S. Doi (1998) Bifurcation in vehicle dynamics and robust front wheel steering control, *IEEE Transactions on Control Systems Technology* 6, 412-420.
- [15] Van der Schaft, A. (1992).  $L_2$ -gain analysis of nonlinear systems and nonlinear  $\mathcal{H}_\infty$  control. *IEEE Trans. Automat. Contr.* 37, 770-784.
- [16] H.D. Tuan, S. Hosoe (1996), On linearization technique in robust nonlinear  $\mathcal{H}_\infty$  control, *Systems and Control Letters* 26, 21-27.
- [17] H.D. Tuan, S. Hosoe (1997), On robust and  $\mathcal{H}_\infty$  controls for a class of linear and bilinear systems with uncertainty, *Automatica* 33, 1373-1377.
- [18] H.D. Tuan, P. Apkarian, Relaxation of parameterized LMIs with control applications, *International J. of Nonlinear Robust Controls* 9(1999), 59-84..
- [19] M. Yamashita, K. Fujimori, C. Uhlik, R. Kawatani and H. Kimura (1990).  $\mathcal{H}_\infty$  control of an automotive active suspension. *Proc. of 29-nd CDC*, 2244-2250.
- [20] F. Wu, X.H. Yang, A.K. Packard, G. Becker, Induced  $L_2$  norm control for LPV systems with bounded parameter variation rates, *Int. J. of Nonlinear Robust Control* 6(1996), 983-998.

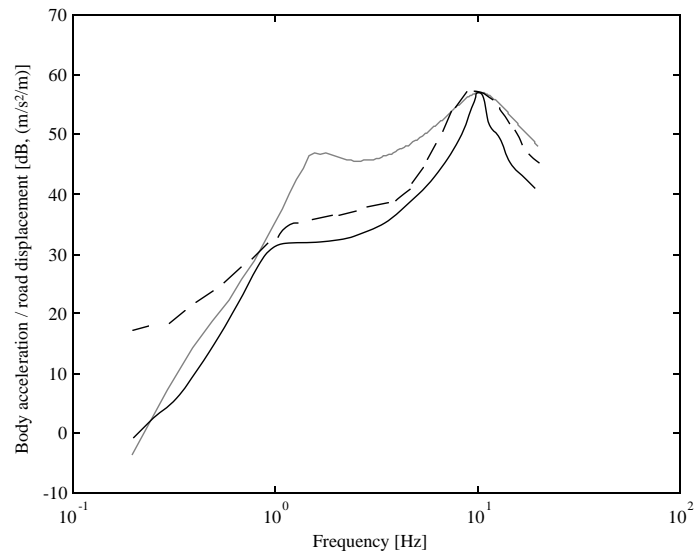


Figure 3: Frequency responses of the simulation results: Nonlinear  $\mathcal{H}_\infty$  control (solid), linear  $\mathcal{H}_\infty$  control for feedback linearized model (dashed) and passive (grey).

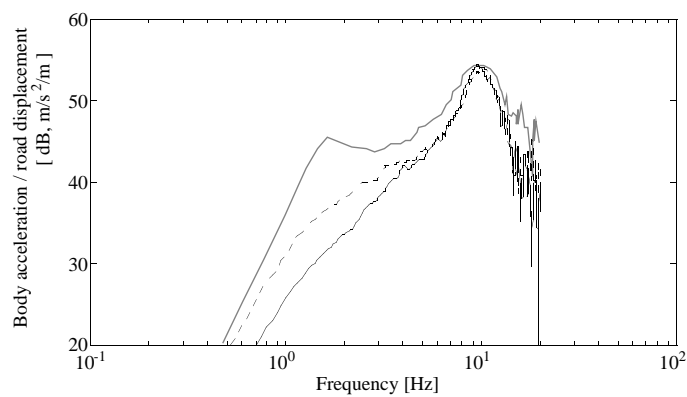


Figure 4: Frequency responses of the experimental results: Nonlinear  $\mathcal{H}_\infty$  control (solid), linear  $\mathcal{H}_\infty$  control for the feedback linearized model (dashed) and passive (grey).

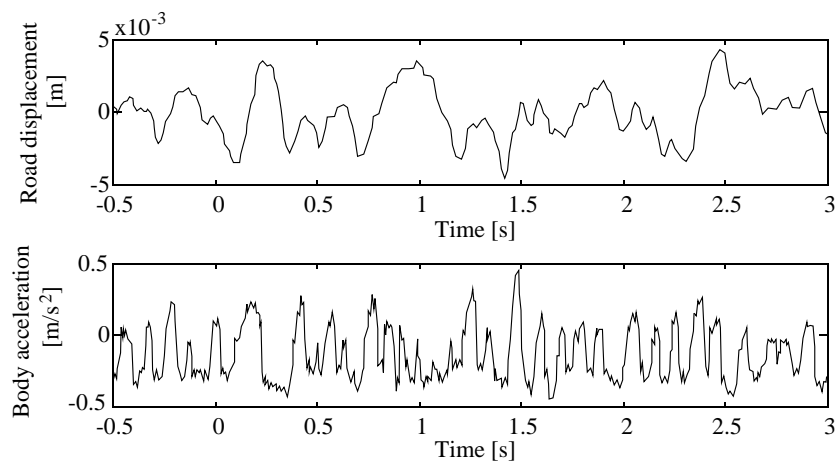


Figure 5: Road displacement and body acceleration with nonlinear  $\mathcal{H}_\infty$  control.

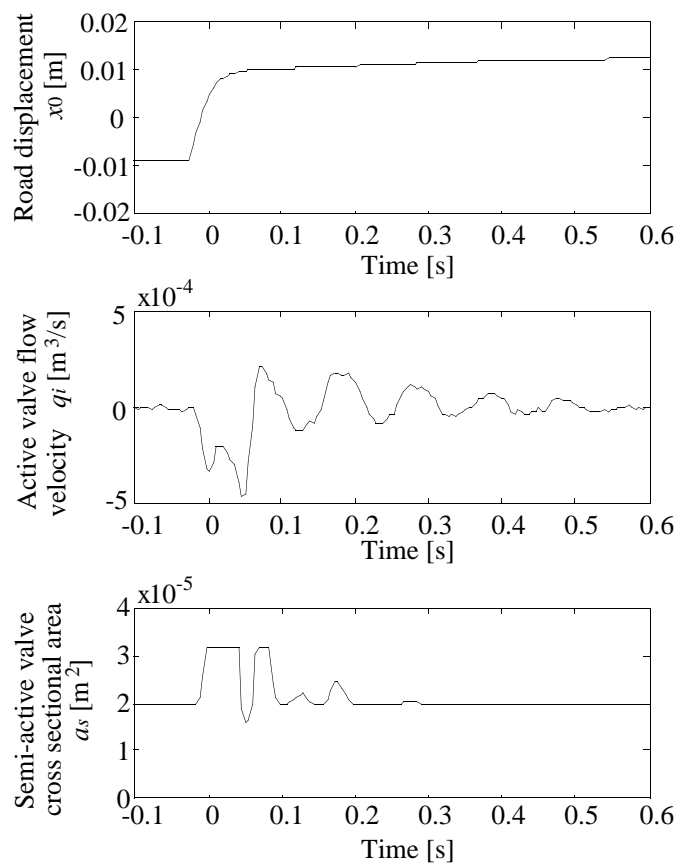


Figure 6: Responses of the active valve flow velocity  $q_i$  (active control input) and the semi-active valve cross sectional area  $a_s$  (semi-active control input) after step disturbance with the nonlinear  $\mathcal{H}_\infty$  control.



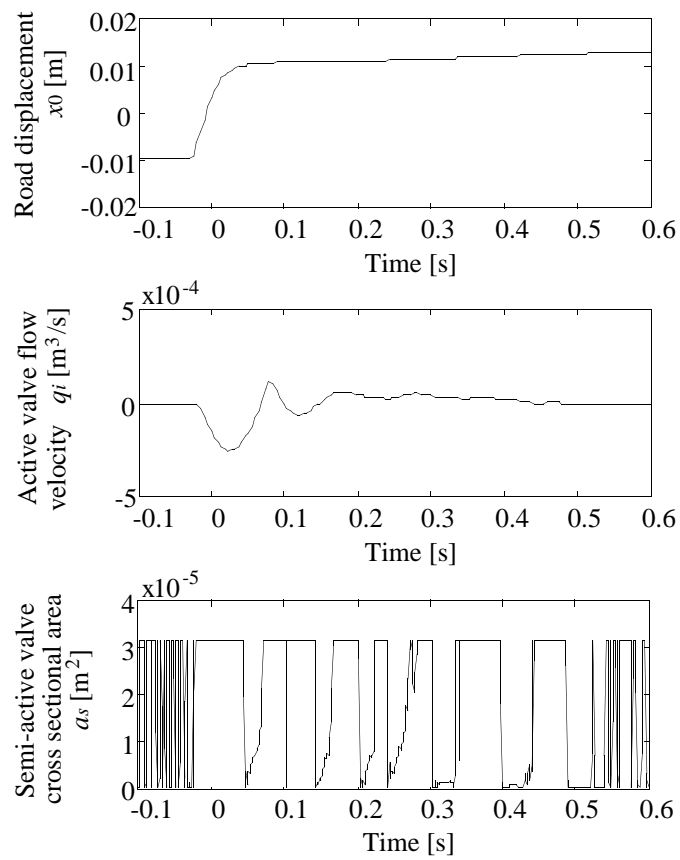


Figure 7: Responses of the active valve flow velocity  $q_i$  (active control input) and the semi-active valve cross sectional area  $a_s$  (semi-active control input) after step disturbance with the linear  $\mathcal{H}_\infty$  control for the feedback linearized model.

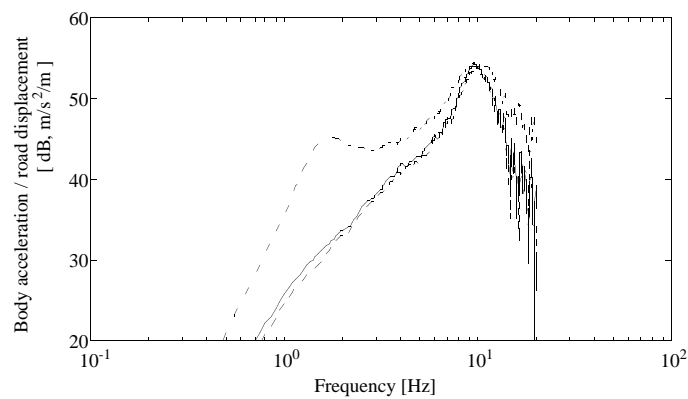


Figure 8: Ride comfort performance of nonlinear  $\mathcal{H}_\infty$  control (at  $\omega_{se} = 0.0015$  (solid) and  $\omega_{se} = 0.0005$  (dashed)) and passive control (dash-dot).

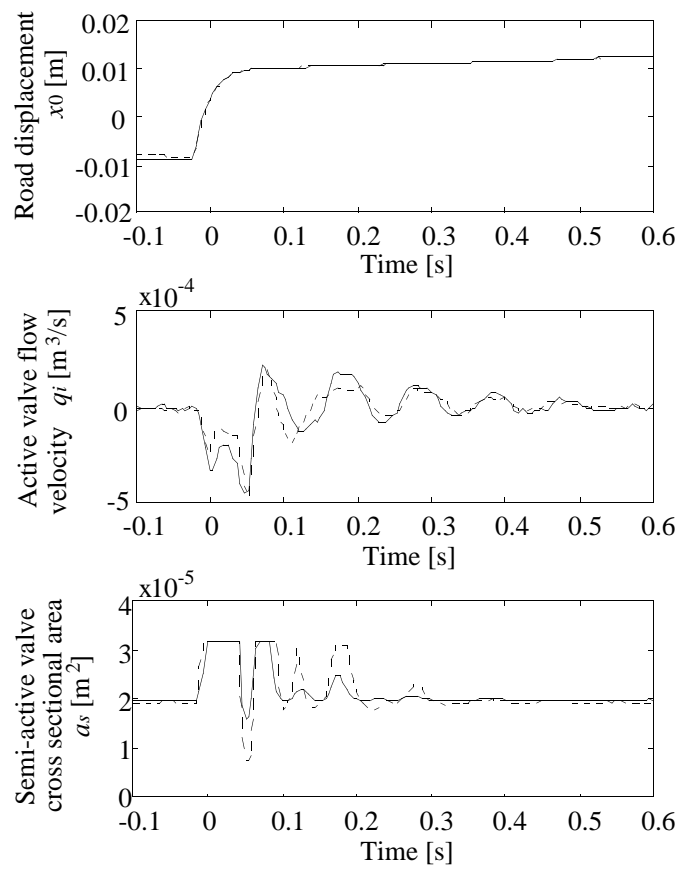


Figure 9: Change of the weighting constant  $\omega_{se} = 0.0015$  (solid) and  $\omega_{se} = 0.0005$  (dashed) for semi-active control input  $u_s$ .

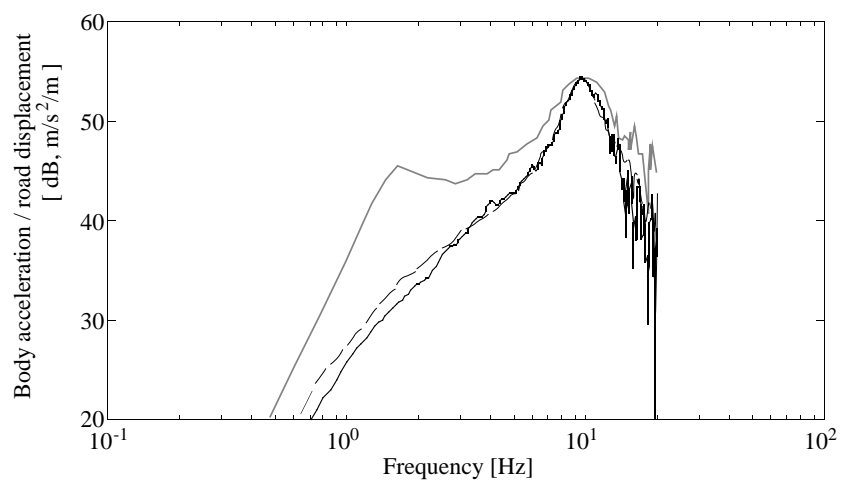


Figure 10: Frequency characteristics of experimental results: the integrated suspension (solid), the pure active suspension (dashed) and passive suspension (grey).

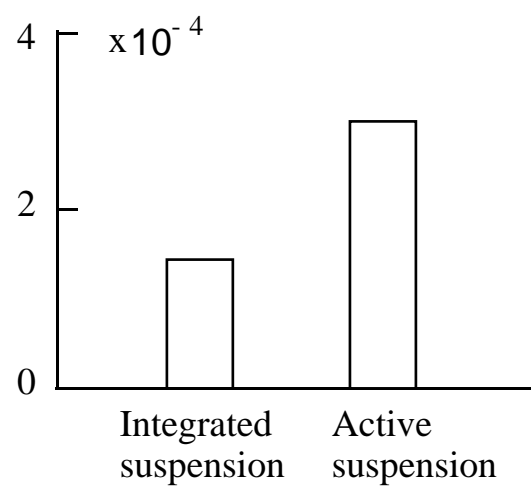


Figure 11: Active oil consumption during 20 seconds.